Review on theory and applications of wavefront recording plane framework in generation and processing of digital holograms

P. W. M. Tsang[1*] and T.-C. Poon[2]

[1]*Department of Electronic Engineering, City University of Hong Kong, Hong Kong SAR, China*

[2]*Bradley Department of Electrical and Computer Engineering, Virginia Tech, Blacksburg VA 24061, USA*

*Corresponding author: eewmtsan@cityu.edu.hk

The wavefront recording plane (WRP), subsequently generalized to be known as the virtual diffraction plane (VDP), is a recent concept that has been successfully deployed in fast generation and processing of digital holograms. In brief, the WRP and its extension, the VDP, is a hypothetical plane that is located between the hologram and the object scene, and which is at close proximity to the latter. As such, the fringe patterns on the hypothetical plane are carrying the holistic information of the hologram, as well as the local optical properties of the object scene. This important property enables a hologram to be processed with classical image processing techniques that are normally unsuitable for handling holographic information. In this paper we shall review a number of works, that have been developed based on the framework of the WRP and the VDP.

OCIS codes: 090.0090, 090.1995, 090.1760.

doi: 10.3788/COL201311.010902.

1. Introduction

Holography is a classical technique for recording the wavefront of a three-dimensional (3-D) scene on a two-dimensional (2-D) image. Dating back a few decades ago, the process can only be conducted through optical means by mixing the object wave with a reference beam, and recording the resulting fringe pattern on a photographic film. With the rapid advancement of computing technologies in recent years, the optical hologram formation mechanism can be simulated with numerical means. Such approach, commonly referred to as computer generated holography (CGH)[1], computes the diffraction pattern emitted from a 3-D object, and adds a reference wave to produce a digital hologram. The latter can be displayed on electronic addressable devices (e.g., spatial light modulator (SLM))[2], or printed with laser[3] or fringe printers[4], and subsequently reconstructed upon suitable illumination to display the 3D scene. Apparently, as a lot of researchers have anticipated that digital holography is likely to become one of the promising solutions in the next generation 3-D display technology. At the same time, such optimism is masked by a number of problems which are difficult to solve in the foreseeable future. A lot of these problems could be traced back to the fine pixel size of a hologram, which is in the order of the wavelength of light. For example, a small 10×10 (mm) hologram with a square pixel size of 5×5 (μm), is comprising of over 4×10^6 points which is over 2 times the number of pixels in a domestic high definition television ($1\,920 \times 1\,080$ (pixel)). One can easily imagine the enormous amount of computation that will be required to generate, or to process a digital hologram with a reasonable display area. Apart from the computation issue, implementation of high resolution holographic display is both expensive and tedious. Lately, a new technology[4−8], which integrates active tiling with

an optical addressed SLM (OASLM), has been reported to overcome this problem. In this method, the fringe pattern of a digital hologram is evenly partitioned into non-overlapping square tiles. A single SLM is employed to cast the diffraction pattern of each tile sequentially onto the corresponding position of an optical recording material. A complete hologram is formed after all the tiles have been recorded. Although the display problem may have been partially alleviated, the formidable amount of computation associated with the generation and processing of the enlarged digital hologram is escalated at the same time.

In this paper, we review a series of research works that are developed based on a modern framework of digital holography known as the wavefront recording plane (WRP), which is subsequently generalized to be known as the virtual diffraction plane (VDP). The concept and theory of WRP are first proposed by a group of researchers for fast generation of digital holograms[9,10]. Different from traditional approaches (for example, Refs. [11–13]) that aims at enhancing the speed of generating a hologram directly from an object scene, the WRP approach converts the latter into a VDP that is located very near to the object scene. Due to the close proximity, the wave emitted from each object point will only cover a small, localized area on the VDP (in contrast with the wave projected onto the hologram, which covers the entire area). As a result, the overall diffraction pattern on the VDP, which is the summation of the contribution of individual object points, can be deduced with very small amount of computation. Subsequently, the VDP can be easily expanded into the ultimate hologram which is further away from the object scene. Experimental evaluation has demonstrated that the WRP method is effective in generating medium size hologram at multiple frames per second, which is fast enough for a holographic video system. The encouraging findings of the WRP frame-

work have also cast light on the possibility of real time holographic signal processing. The rationale is that the VDP is found to carry the diffraction fringes of the entire hologram, but at the same time similar optical properties as the object scene. Grossly speaking, this implies that modifying the brightness and contrast on the VDP will lead to almost identical changes on the pictorial contents it represents. Along this line of thinking, if a hologram can be reverted into a VDP, the latter can be conveniently processed with a lot of existing image processing techniques and tools.

Organization of the article is given as follows. In section 2, for the sake of clarity, the fundamental principles of CGH is outlined. Next, the works in Refs. [9,10,14], which employs the WRP framework to speed up the computing of the hologram, is described. In section 3, we shall extend the WRP framework into the VDP framework to illustrate some post-processing of holographic information. A number of case studies on hologram processing based on the VDP framework, reported in Refs. [15,16], are described in section 4. This is followed by a conclusion summarizing the essential findings.

2. Concept of WRP framework and its application in CGH

2.1. Fundamental principles of CGH

To start with, we would like to provide a brief introduction on CGH. Consider a 3-D object surface comprising of N self-illuminating points. The intensity of each point, and its axial distance (depth) from the hologram are given by a_j and dp_j, respectively. The complex Fresnel $H(x,y)$ can be mathematically described as[1]

$$ H(x,y)\Big|_{\substack{0 \leqslant x < X \\ 0 \leqslant y < Y}} = \sum_{j=0}^{N-1} \frac{a_j}{r_j} \exp\left(\mathrm{i}\frac{2\pi}{\lambda}r_j\right), \quad (1) $$

where X and Y are the horizontal and vertical extents of the hologram, respectively, and are assumed to be identical to that of the object scene; λ is the wavelength of the optical beam which is used to generate the complex hologram. The term $r_j = \sqrt{(x-x_j)^2 + (y-y_j)^2 + dp_j^2}$ is the distance of an object point at position (x_j, y_j) to a point at (x,y) on the hologram. From Eq. (1), we can see that each object point is contributing to the entire hologram, and the evaluation of each hologram pixel involves the complicated expression enclosed in the summation operator.

2.2. Fast generation of CGH based on the WRP framework[9,10]

In simple terms, a WRP is a hypothetical plane that is parallel to the hologram, and placed at close proximity to the object scene. The spatial relation between the object scene, the WRP and the hologram is shown in Fig. 1. It can be seen that wavefront emitted from a self-illuminating point will diverge to cover the entire hologram, and intercept the WRP in its path. From Fig. 1, it can be inferred that if the WRP is near to the object point, the coverage of the object wavefront on the hypothetical plane is limited to a small virtual window.
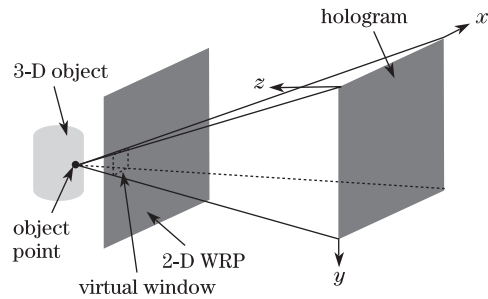
Fig. 1. Spatial relation between the 3-D object space, the 2-D WRP, and the hologram.

For simplicity of visualization and implementation, the virtual window is assumed to be a square region of size $W \times W$. The Fresnel diffraction equation in Eq. (1) can be applied, with slight modification, to compute the diffraction pattern $u_{\mathrm{w}}(x,y)$ on the WRP. Let d_j denote the axial distance from the jth object point to the WRP, we have

$$ u_{\mathrm{w}}(x,y)\big|_{(x,y)\in VW_j} = \sum_{j=0}^{N-1} \frac{a_j}{R_{\mathrm{w}j}} \exp\left(\mathrm{i}\frac{2\pi}{\lambda}R_{\mathrm{w}j}\right), \quad (2) $$

where $R_{\mathrm{w}j} = \sqrt{(x-x_j)^2 + (y-y_j)^2 + d_j^2}$ is the distance of the point from the WRP, and VW_j denotes the corresponding virtual window. Equation (2) can be rewritten as

$$ u_{\mathrm{w}}(x,y) = \sum_{j=0}^{N-1} F_j(x,y), \quad (3) $$

where

$$ F_j(x,y) = \begin{cases} \dfrac{A_j}{R_{\mathrm{w}j}} \exp\left(\mathrm{i}\frac{2\pi}{\lambda}R_{\mathrm{w}j}\right) & \text{if } |x-x_j| \text{ and } |y-y_j| < \frac{1}{2}W \\ 0 & \text{otherwise.} \end{cases} $$

In Eq. (2), the computation of the WRP for each object point is only confined to the region of the virtual window on the WRP. As W is much smaller than X and Y, the computation load is significantly reduced as compared with Eq. (1). In Ref. [9], the calculation is further simplified by pre-computing the exponential terms $\exp\left(\mathrm{i}\frac{2\pi}{\lambda}R_{\mathrm{w}j}\right)/R_{\mathrm{w}j}$ for all combinations of $|x-x_j|$, $|y-y_j|$, d_j (within the coverage of the virtual window), and storing the results in a look up table (LUT). The estimated computational amount is $2\alpha N\bar{L}^2$, where $\bar{L}$ is the mean perpendicular distance of the object points to the WRP, and α is the arithmetic operations involved in computing the wavefront contributed by each object point. With the use of the LUT to retrieve the value of the exponential term in Eq. (2), computation of $F_j(x,y)$ only involves one multiplication operation for each point within the virtual window. If the latter is a square comprising of 64×64 (pixel), the derivation of the diffraction pattern for each virtual window will only involve 4 096 multiplication operations.

In the second stage, the WRP is expanded to the hologram as

$$ u(x,y) = K\mathcal{F}^{-1}\left\{\mathcal{F}[u_{\mathrm{w}}(x,y)] \cdot \mathcal{F}[h(x,y)]\right\}, \quad (4) $$

where $\mathcal{F}[\cdot]$ and $\mathcal{F}^{-1}\{\cdot\}$ denote the forward and inverse Fourier transform, respectively; $K = -\frac{\mathrm{i}}{\lambda z_{\mathrm{w}}}\exp\left(\mathrm{i}\frac{2\pi z_{\mathrm{w}}}{\lambda}\right)$

is a constant and $h\left(x,y\right) = \exp\left(\mathrm{i}\frac{\pi}{\lambda z_{\mathrm{w}}}\left(x^2 + y^2\right)\right)$ is an impulse function which is fixed for a given separation z_{w} between the WRP and the hologram.

In Eq. (4), the term $\mathcal{F}\left[h\left(x,y\right)\right]$ can be pre-computed in advance, and hence it is only necessary to compute the forward and the inverse Fourier transform operations. Both processes can be conducted swiftly with graphic processing unit (GPU). The WRP method results in significant improvement over the speed in generating the hologram, as the computation of the wavefront from each object point is only restricted to a small $W \times W$ virtual window. As demonstrated in Ref. [9], a video sequence of digital holograms, each comprising of $2\,048{\times}2\,048$ (pixel) and representing 10^4 object points, can be generated at a rate of 10 frames per second. Lately, the method has been extended to generate a hologram from an object scene that is larger than the hologram with the use of the Shifted-Fresnel diffraction[17].

2.3. Fast generation of CGH for a 3-D surface based on the interpolative wavefront recording method[14]

Adopting the WRP framework, Tsang *et al*. has proposed an enhanced method, known as the interpolative wavefront recording method[14], to speed up the hologram generation method, and extended it to handle a 3-D object surface which has the same size and number of pixels as the hologram. In this approach, the intensity profile of the 3-D surface is denoted by a 2-D function $I\left(x,y\right)$. Each point in $I\left(x,y\right)$ is associated with a depth value $d\left(x,y\right)$ representing its axial distance to the WRP. Furthermore, it is assumed that the scene image should be considerably smaller in resolution than that of the hologram, which is generally true in practice. As such, object points that are clustered around a small neighborhood will share similar optical and spatial properties. On this basis, the intensity profile is evenly partitioned into non-overlapping square support of size $M \times M$ as shown in Fig. 2. The object point at the center of the support is taken as a sample point. As an example, the support of an object point at $\left(x_m,y_n\right)$, bounded by the vertical margins t_n and b_n, and the horizontal margins l_m and r_m, is shown in Fig. 2. Within each square support, all the pixels are assumed to have identical intensity and depth value as the sample point in the center of the square. This is equivalent to down-sampling the object scene with a factor of M along the vertical and horizontal directions, and filling the empty gaps between the sample points with padding. The term WRP that records the wavefront from the interpolated object scene is therefore referred to as the "interpolative wavefront recording plane" (IWRP).

Due to the close proximity of the IWRP and the object scene, the wavefront projected from a support of pixels will only cover a small virtual window, which is practically similar in size and location as the support, on the WRP as shown in Fig. 3. Similar to the support of the object points, the virtual windows are non-overlapping with each other. We first consider a virtual window corresponding to an object point at the origin, with intensity and depth equal to e and f, respectively. The diffraction wave within the virtual window, centered at

$\left(0,0\right)$, is given by

$$G_{\mathrm{A}}\left(x,y,e,f\right)_{\mathrm{center}=(0,0)} = e \sum_{\tau_x=-\frac{M}{2}}^{\frac{M}{2}-1} \sum_{\tau_y=-\frac{M}{2}}^{\frac{M}{2}-1}$$

$$\cdot \exp\left[\mathrm{i}2\pi R_f\left(x - p\tau_x, y - p\tau_y\right)/\lambda\right], \tag{5}$$

where p is the separation between adjacent pixels; $R_f\left(x,y\right) = \sqrt{x^2 + y^2 + f^2}$ is the distance of the sample object point at the center of the support to the location $\left(x,y\right)$ on the WRP; τ_x and τ_y are integers denoting the pixel shift along the horizontal and vertical directions, respectively. It can be inferred from Eq. (5) that for an object point that is not located at $\left(0,0\right)$, say at $\left(x_m,y_n\right)$ in the example shown in Fig. 2, the diffraction pattern is simply a shifted version of the one at the origin, i.e.,

$$G_{\mathrm{A}}\left(x,y,e,f\right)_{\mathrm{center}=(x_m,y_n)}$$
$$= G_{\mathrm{A}}\left(x - x_m, y - y_n, e, f\right)_{\mathrm{center}=(0,0)}, \tag{6}$$

with $e = I\left(m,n\right)$ and $f = d\left(m,n\right)$ is the axial distance of an object point at $\left(m,n\right)$ to the hologram.

From Eq. (6), it can be seen that $u_{\mathrm{w}}\left(x,y\right)$ can be expressed as a function that is the union of the non-overlapping virtual windows of all the sample object
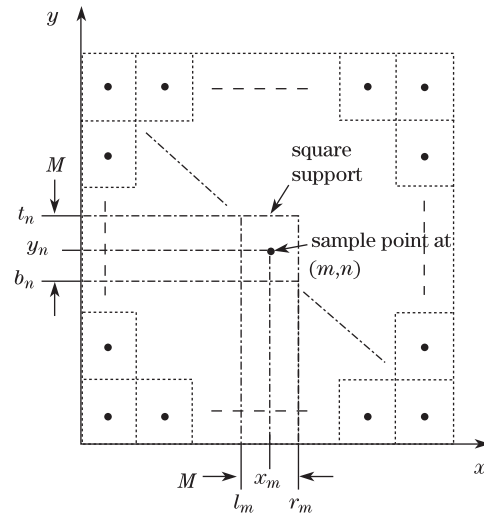
Fig. 2. Partitioning of the object scene into non-overlapping square support (excerpted from Ref. [14]).
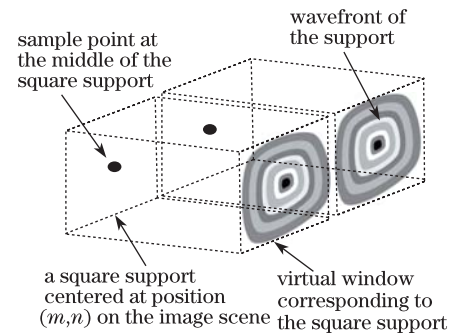
Fig. 3. Spatial relation between the square support and its corresponding virtual window.

points, as given by

$$u_\text{w}(x,y) = \underset{m,n}{\cup} G_\text{A}(x-x_m, y-y_n, I(m,n), d(m,n)),$$
(7)

where m and n are indices of the sample points at positions (x_m, y_n).

We further note that the diffraction pattern $G_\text{A}(x, y, e, f)_{\text{center}=(0,0)}$, that is bounded within the virtual window, can be pre-computed for all valid combinations of e and f, and store in a LUT. Consequently, the content of each virtual window in the IWRP can be retrieved, from the LUT, the wavefront corresponding to the intensity and depth of the corresponding object point. As such, derivation of the wavefront on the IWRP can be conducted in a computation-free manner.

From Fig. 3, it can be inferred that the object wave on the WRP can be obtained simply by tiling the virtual windows, each containing the diffraction fringes of its corresponding support. Being different from the computation of the WRP with the parent method[9,10] (Eq. (4)), there is no need to accumulate the diffraction pattern and the process is near computational free in practice. Subsequently, Eq. (4) is applied to expand the WRP into a full hologram. The method, implemented with GPU, is capable of generating hologram representing an object of over 10^6 points at over 40 frames per second.

3. Post-processing of holographic information based on the VDP method

Being similar to optical images, the quality of the pictorial contents represented in a digital hologram may not meet the desired expectation of different observers. The problem is even more severe if the digital hologram is acquired optically, where it is difficult, if not impossible, to control the illumination in the capturing process. In addition, some of the image scenes are inherently poor in appearance, lacking of sufficient brightness, contrast, and sharpness to reveal the fine details of their ingredients. These kind of unfavorable factors generally result in artifacts such as overexposure, underexposure, and blurriness, in the reconstructed images. In traditional photography, the defects can be easily alleviated by readjusting the intensity of individual pixels. To date, there are numerous handy software programs and image processing techniques that have been developed on such basis, and which could effectively rectify most of the visual degradation. However, it can be inferred from Eq. (1) that such approach cannot be applied with equal success to a digital hologram, as each pixel in the hologram is contributed from all the object points in the scene. In another words, modifying a single hologram pixel will lead to a change in the entire scene, instead of clustering around the neighborhood of the pixel. Intuitively, it is possible to recover the original 3-D scene from the hologram, and apply some classical image processing algorithms to improve the optical properties. Subsequently, the corrected image scene can be re-converted to a hologram. The loophole in this straightforward approach is that so far there is no effective method for recovering a generic 3-D object scene from a digital hologram. Until now, only images of lines and simple geometries, could

be extracted from the hologram[18,19]. Besides, even with such constraint, the processes involved in these methods are both complicated and computationally intensive. In this section, the principles of digital hologram processing based on the WRP (VDP) framework, is first described. Next, we shall report a number of fast methods that employ the WRP (VDP) framework for modifying or enhancing the pictorial contents represented in a digital hologram.

3.1 Digital hologram processing based on the VDP framework

The principle of VDP-based holographic information processing, which can be divided into 3 stages, is depicted in Fig. 4.

In the first stage, digital hologram $H(x,y)$ is first back-projected onto the VDP that is placed near to the object scene. Referring to Fig. 1, it can be seen that for each object point, the entire hologram will be back-projected into a small virtual window on the WRP.

Suppose the VDP is located at an axial distance z_w from the hologram, and the complex wavefront $u_\text{w}(x,y)$ on the VDP is given by the convolution between $H(x,y)$ and the free-space spatial impulse response $g(x,y)$ as

$$u_\text{w}(x,y) = H(x,y) * g(x,y),$$
(8)

where $g(x,y) = K^* h^*(x,y)$. Denoting $\mathcal{F}[\cdot]$ and $\mathcal{F}^{-1}\{\cdot\}$ to be the forward and inverse fast Fourier transform (FFT) operations, respectively, the convolution in Eq. (8) can be expressed in the frequency domain as

$$u_\text{w}(x,y) = \mathcal{F}^{-1}\{\mathcal{F}[H(x,y)] \cdot \mathcal{F}[g(x,y)]\}.$$
(9)

In the second stage, selected region(s) on the VDP, denoted by S, is processed with a given function $P[\cdot]$. After the modification, the diffraction pattern on the VDP becomes

$$v_\text{w}(x,y) = \begin{cases} P[u_\text{w}(x,y)] & (x,y) \in S \\ u_\text{w}(x,y) & \text{otherwise} \end{cases}.$$
(10)

In the third stage of the VDP processing framework, the modified wavefront is forward projected to become a modified hologram given by

$$H_\text{P}(x,y) = v_\text{w}(x,y) * g^*(x,y).$$
(11)

The forward projection process can be realized in the frequency spectrum, and we have

$$H_\text{P}(x,y) = \mathcal{F}^{-1}\{\mathcal{F}[v_\text{w}(x,y)] \cdot \mathcal{F}[g^*(x,y)]\}.$$
(12)

In Eqs. (9) and (12), the FFT of $g(x,y)$ and $g^*(x,y)$ can be pre-computed in advance. Hence, the processing of a hologram with the VDP framework mainly involves a pair of forward and inverse FFT operations. The rest of the processes are negligible in computation time. Based on a commodity GPU to conduct the FFT, a medium size digital hologram comprising of $2\,048 \times 2\,048$ (pixel) can be processed in less than 10 ms, equivalent to a rate of over 100 frames per second.
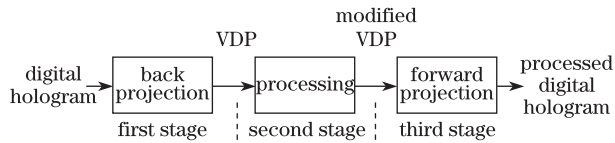
Fig. 4. Hologram processing based on the VDP framework.

4. Case studies on hologram processing based on the VDP framework

4.1. Hologram relighting[15]

In this section, we shall review a number of methods that have been reported in Refs. [15,16] for processing the pictorial content of digital holograms based on the VDP framework.

Relighting is a simple way of readjusting the illumination effect in a picture. In classical image processing, this can be accomplished simply by modulating an image with a relighting function that modifies the optical properties of individual pixels. As explained previously (as well as illustrated in Ref. [15]), this straightforward approach is not applicable directly to a hologram as each pixel is affecting the entire object scene instead of its neighborhood. However, the holistic property of pixels is not significant in the domain of the VDP, as each pixel is only representing a very small number of points in the object scene. As such, the relighting process can be applied to the VDP of a hologram. Mathematically, this can be realized by adopting a modulating function for $P[\cdot]$ in Eq. (10), as given by

$$v_{\mathrm{w}} = P[u_{\mathrm{w}}(x,y)] = u_{\mathrm{w}}M(x,y), \qquad (13)$$

where $M(x,y)$ is a relighting mask. Subsequently, the processed VDP is forward projected to the digital hologram based on Eq. (12).

The VDP relighting method can be demonstrated with the hologram of the double depth image in Fig. 5(a), together with a relighting mask simulating a slanting, directional illumination emerging from the upper right corner as shown in Fig. 5(b). The image is evenly partitioned into a left side and a right side, located at 0.5 and 0.6 m from the hologram, respectively. A digital Fresnel hologram is generated with Eq. (1) based on the optical setting in Table 1.

The numerical reconstructed images at the two depth planes are shown in Figs. 5(c) and (d). It can be seen that the focused part of each reconstructed image is similar to the original content. Next, the relighting mask $M(x,y)$ in Fig. 5(b) is employed to relight the VDP. The reconstructed images of the relit hologram at the two focal planes are shown in Figs. 5(e) and (f). We observed that the desired illumination effect is attained.

4.2. Hologram enhancement based on histogram equalization[16]

Being similar to classical photography, certain part(s) of the object scene represented in a digital hologram may be over-exposed or under-exposed, resulting in a poor visual impression. Intuitively, such defects can be alleviated with the VDP framework, by applying a relighting mask on the
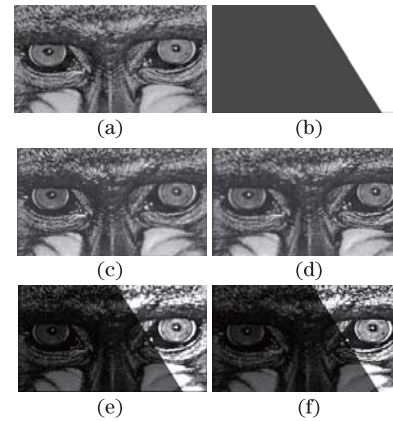
Fig. 5. (a) Scene image evenly divided into a left and a right sections, positioned at 0.5 m and 0.6 m from the hologram plane, respectively; (b) relighting image simulating the directional illumination emerging from the upper right corner; numerical reconstructed images of the digital hologram representing the scene image in (a) at focal distances of (c) 0.58 m and (d) 0.6 m, respectively; numerical reconstructed images of the digital hologram representing the image in (a), that has been relight with our proposed method based on the relighting image in (b), at focal distances of (e) 0.5 m and (f) 0.6 m, respectively. Figures 5(a)–(f) excerpted from Ref. [16]

Table 1. Optical Setting Adopted in the Hologram Generation Process

Hologram Size (pixel)	$2\,048 \times 2\,048$
Pixel Size of the Hologram (μm^2)	7
Wavelength of Light (nm)	650

VDP to inhibit the brightness and contrast of the over-exposed region(s), and magnify the under-exposed ones. However, in practice it will be extremely tedious and time consuming to design a suitable relighting mask to compensate these kinds of defects. To overcome this problem, a solution has been reported in Ref. [16], and described as follows. To begin with, over and under-exposure of an image scene can be attributed to an uneven probability distribution of the pixel intensities. Due to the similarity in optical properties between the object scene and the VDP, both domains also share similar probability distributions on the pixel intensities. On this basis, the defects are compensated by applying histogram equalization[20], a technique which is widely employed in enhancing optical images, to the VDP. The histogram $p(m)$ representing the probability density function of the magnitude of the pixel values in the VDP, which have been normalized to the range [0,1], is computed first. Suppose there are M pixels in the VDP, and $N(m)$ is the number of pixels with magnitude equals to m, the histogram is given by

$$P(m) = N(m)/M. \qquad (14)$$

From Eq. (14), the cumulative distributive function is deduced as

$$cdf(i) = \sum_{k=0}^{i} P(k). \qquad (15)$$

Based on the cumulative distributive function, a mapping function is derived to convert the magnitude of each pixel value (with original value 'm') to a new quantity 'n'

between the interval (0,1). Suppose D is the maximum pixel value, we have

$$n = D \times cdf(m)|_{m>0}. \qquad (16)$$

From Eq. (16), we obtain a re-scaling function given by

$$T(m)|_{m>0} = n/m. \qquad (17)$$

Next, a relighting mask is generated based on $T(m)$ as

$$M(x,y) = T(|u_w(x,y)|). \qquad (18)$$

The enhancement method is demonstrated with a $1\,920 \times 960$ double depth image in Fig. 6(a). The image is evenly partitioned into a left side and a right side, located at 0.56 m and 0.6 m from the hologram, respectively. The picture is underexposed in most of the area, but overexposed along the rim of the nose. Equation (1) is applied to generate a $2\,048 \times 2\,048$ digital hologram based on the optical settings in Table 1, and the numerical reconstructed images at the two depth planes are shown in Figs. 6(b) and (c). When either side of the reconstructed image is in focus, it is a good recovery of the original content. The digital hologram is converted into a WRP that is located at an axial distance of 0.58 m from the hologram (i.e., halfway between the 2 focal planes). The VDP is relit with the mask derived from Eqs. (14)–(18), and forward projected to a digital hologram. The reconstructed images at the two depth values are shown in Figs. 6(d) and (e). We observe that in the reconstructed images, the brightness and contrast in the over and under-exposed areas are improved.

4.3. Hologram sharpening based on high-boost filtering[16]

Apart from readjusting the brightness and contrast of the image represented in a hologram, sometimes it is also necessary to enhance the sharpness in certain region to increase the visibility of the high frequency contents. Based on the VDP framework, this process can be achieved by applying a high-boost filter to the selected area on the VDP of a hologram, as given by

$$v_w(x,y)|_{(x,y)\in R} = A[u_w(x,y) - Bu_w^L(x,y)], \qquad (19)$$

where $u_w^L(x,y)$ is a low-pass version of R. Each pixel in $u_w^L(x,y)$ is derived from the average value of a 3×3 window centered at the corresponding pixel according to

$$u_w^L(x,y) = \frac{1}{9} \sum_{m=-1}^{1} \sum_{n=-1}^{1} u_w(x+m, y+n). \qquad (20)$$

The terms A and B are constant values. The larger the values of A and B, the higher will be the brightness and sharpness of the region R, respectively. Other types of sharpening filters can be applied under the same principle.

The hologram sharpening process is illustrated with
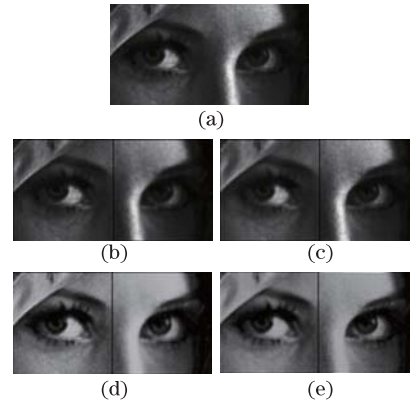
Fig. 6. (a) Scene image evenly divided into a left and a right sections, positioned at 0.56 m and 0.6 m from the hologram plane, respectively; (b) and (c) are numerical reconstructions of the hologram representing the double depth planes at 0.56 m and 0.6 m, respectively; (d) and (e) are numerical reconstructions of the hologram representing the double depth values at 0.56 m and 0.6 m, respectively. The hologram has been enhanced with histogram equalization on the VDP. Figures 6(a)–(e) excerpted from Ref. [16]
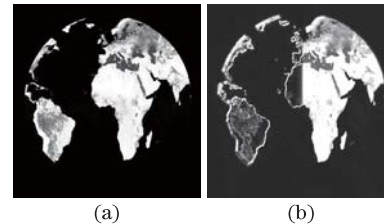
Fig. 7. (a) Original image of a hemisphere with the texture of an earth image positioned at 0.3 m from the hologram plane. The radius of the hemisphere is 5 mm; (b) numerical reconstructed image of the hologram representing the image in (a) after application of high-boost-filtering to sharpen the left side of the globe on the VDP. Figures 7(a) and (b) excerpted from Ref. [16]

a hemisphere with the texture of the earth image as shown in Fig. 7(a). The hemisphere has a radius of 5 mm with its tip located at 0.3 m from the hologram. Equation (1) is applied to generate the hologram of the hemisphere, and the VDP is obtained with Eq. (9). The high-boost-filter in Eq. (20) is applied to the VDP, and subsequently forward projected into a hologram. The reconstructed image of the modified hologram, focused at 0.3 m (causing slight de-focusing around the rim of the hemisphere, which will become more apparent when the figure is zoomed in), is shown in Fig. 7(b). It can be seen that the edges on the left side of the image of reconstructed image is strengthened, and the rest of the reconstructed image is not affected.

5. Conclusion

In this paper, we report a number of recent works that employs the WRP framework for fast generation and the VDP framework for processing of digital holograms. The WRP can be interpreted as a virtual holographic plane that is placed between the digital hologram and the object scene, close to the latter, and carrying the properties in both domains. The works in Refs. [9,10,14] demonstrate that it is significantly faster to generate a WRP, as compared with a digital hologram, from an object scene.

The conversion of the WRP to the hologram, in turns, can be realized swiftly with the use of the GPU. As such, generation of the digital hologram for representing 3-D scene with large number of object points can be conducted at the video rate. The WRP framework has also been extended to the processing of digital holograms. In this approach, the hologram is back-projected onto a VDP that is close to the object scene. Being similar to the WRP, the VDP is also carrying the local optical properties of the object scene, although they are derived from different sources (the former from the object scene, and the latter from the hologram). As such, the pictorial content of a hologram can be modified by processing its corresponding VDP. Based on this principle, a hologram relighting method has been attempted and reported in Ref. [15]. In this approach, the field distribution on the VDP is modulated with a relighting mask to modify the brightness and contrast of selected regions. The VDP is then forward projected to become the hologram. Experimental evaluation revealed that the reconstructed image of the modified hologram is correctly relit by the relighting mask. In addition, the entire process can be conducted at a speed exceeding the video frame rate with a commodity computing device that is equipped with a GPU. This is an important finding as it opens the door for digital hologram to be processed with classical image processing techniques, and without the presence of the original 3-D object scene. In view of the favorable outcome in Ref. [15], the method has been further applied to enhance the brightness and contrast, as well as sharpening selected regions on the pictorial contents represented in a digital hologram. Successful results have been illustrated in Ref. [16], further demonstrating the effectiveness of the WRP framework.

References

1. T.-C. Poon, *Digital Holography and Three-Dimensional Display: Principles and Applications* (Springer, New York, 2006).
2. J. P. Liu, W. Y. Hsieh, T.-C. Poon, and P. Tsang, Appl. Opt. **50,** H128 (2011).
3. L. C. Ferri, Comp. Graph **25,** 309 (2001).
4. H. Yoshikawa and M. Tachinami, Proc. SPIE **5742,** 259 (2005).
5. M. Stanley, Proc. SPIE **5005,** 247 (2003).
6. N. Collings and J. Nonlin, Opt. Phys. Mater. **20,** 453 (2011).
7. C. Slinger, C. Cameron, and M. Stanley, Computer **38,** 46 (2005).
8. H.-S. Lee, H. Song, S. Lee, N. Collings, and D. Chu, in *Proceedings of Coll. Conf. 3D Res. (CC3DR)* 71 (2012).
9. T. Shimobaba, H. Nakayama, N. Masuda, and T. Ito, Opt. Express **18,** 19504 (2010).
10. T. Shimobaba, N. Masuda, and T. Ito, Opt. Lett. **34,** 3133 (2009).
11. S. C. Kim and E. S. Kim, Appl. Opt. **50,** 3375 (2011).
12. P. Tsang, J. P. Liu, K. W. K. Cheung, and T.-C. Poon, Appl. Opt. **48,** H23 (2009).
13. T. Yamaguchi, G. Okabe, and H. Yoshikawa, Opt. Eng. **46,** 125801 (2007).
14. P. Tsang, W. Cheung, T.-C. Poon, and C. Zhou, Opt. Express **19,** 15205 (2011).
15. P. Tsang, K. Cheung, and T.-C. Poon, Opt. Express **20,** 5962 (2012).
16. P. Tsang, T.-C. Poon, and K. Cheung, Opt. Express **20,** 14183 (2012).
17. J. Weng, T. Shimobaba, N. Okada, H. Nakayama, M. Oikawa, N. Masuda, and T. Ito, Opt. Express **20,** 4018 (2012).
18. P. W. M. Tsang, K. W. K. Cheung, T. Kim, Y. S. Kim, and T.-C. Poon, Opt. Lett. **36,** 2650 (2011).
19. X. Zhang, E. Y. Lam, T. Kim, Y. S. Kim, and T. -C. Poon, Opt. Lett. **34,** 3098 (2009).
20. R. C. Gonzales and R. E. Woods, *Digital Image Processing* (Prentice Hall, 2007).